8th Congress of the Alps Adria Acoustics Association
Zagreb, Croatia
20 – 21 September 2018

Hrvatsko akustičko društvo
Acoustical Society of Croatia

LINEARIZED SIMULATIVE APPROACH FOR THE INVESTIGATION OF A FRICTION-INDUCED LOW-FREQUENCY BRAKE MOAN OSCILLATION PHENOMENON WITHIN PASSENGER VEHICLE FRONT AXLES

Severin Huemer-Kals, Manuel Pürscher, Peter Fischer

Graz University of Technology, Institute of Automotive Engineering (FTG)
Inffeldgasse 11/II, 8010 Graz, Austria
Contact: severin.huemer-kals@tugraz.at

Abstract: *Noise, Vibration and Harshness phenomena regarding a passenger vehicle's brake and suspension system can imply a reduced sense of quality as well as significant warranty costs. In contrast to well-researched mid- to high-frequency brake squeal, low-frequency vibrations have gained popularity only most recently. Brake moan is one of these effects, featuring frequencies from 350-600 Hz. Among others, independent wheel suspension systems at the front axle can exhibit moan-related oscillations. Here, evaluations imply high familiarity to disk brake squeal, which can be explained by a coupling of different eigenmodes of suspension and brake system, induced by the frictional contact between disk and pads. Consequently, simulation techniques used for squeal evaluation should be applicable for moan phenomena too. Hence, the linearized approach of the Complex Eigenvalue Analysis was investigated for a Finite Element model of a vehicle's front corner. Parameter variations within a relevant operating range were performed for two different rim designs. A validation based on experimental tests reveals the simulative method's ability to predict the eigenfrequency of characteristic torsional rim oscillations. However, stability was computed divergent to the systems' real-life behaviors: Further examination and correct implementation of sensitive parameters seem necessary for a predictive application of this linearized, simulative approach.*

Key words: brake vibrations, complex eigenvalue analysis, friction-induced vibrations, moan, stability analysis

1. INTRODUCTION

Within a conventional vehicle, the internal combustion engine ensures a certain amount of background noise during driving. For the increasing numbers of Battery Electric (BEV) and Plug-in Hybrid Vehicles (PHEV), this sound source drops out and increases the influence of low-frequency (<1000 Hz) suspension and brake Noise, Vibration and Harshness (NVH) issues. What is more, new driving modes such as automated parking utilize the brakes while a certain drive torque is present at the same time. Because friction-induced low-frequency vibrations essentially occur for the combination of low speed and low brake pressure, as explained in [1, p. 630], their impact on quality and warranty costs is rising.

Brake moan is one of the relevant phenomena, see fig. 1 for an overview. Based on the authors' experience, its main frequency can be found between approx. 350-600 Hz. However, [2] concatenates results from several studies to an even wider range of 200-1000 Hz.

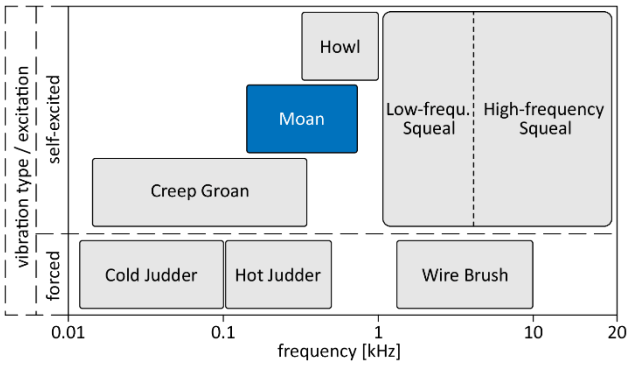

Fig. 1. Brake NVH phenomena classified by vibration type and first dominant frequency, adapted from [3–8]

The exact excitation mechanism of this NVH effect, induced by the frictional contact between the rotating brake disk and the brake pads, is still not perfectly clear. Whereas some researchers refer to the stick-slip effect, e.g. [9, p. 1392, 10, p. 1, 11], others claim modal coupling similar to brake squeal to be responsible, see e.g. [2, 12]. Supporting the authors' opinion given in [13], the research

group of [2] states that this discrepancy could probably relate to the distinction by frequency: Depending on each individual axle's stiffness and mass parameters, either "global" stick-slip transitions – i.e. breakaway throughout the whole pad/disk contact – or modal coupling can lead to NVH issues in a similar frequency range.

Brake moan is mostly known to occur at a car's rear axle: E.g., [2] explains a moan phenomenon at a twist-beam suspension setup. Operational deflections were dominated by rotations of the caliper about its vertical axis, the vehicle roll axis and the wheel axis. Furthermore, a coupling between left and right brake system was discovered. For front axle systems with double wishbone suspension, [14] describes a torsional rim mode in combination with control arm bending oscillations.

Similar to the well-researched, higher-frequency brake squeal, frequency analyses typically show a distinct first peak accompanied by several superharmonic contents of lower energy, see e.g. [15, p. 5]. An example is given by the frequency plot of measured brake pad accelerations in fig. 2.

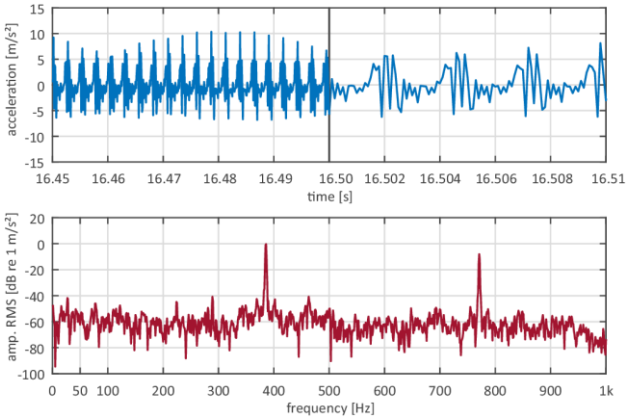

Fig. 2. Longitudinal pad acceleration during 386 Hz moan, adapted from [13, 16]

Similar to other applications within the automotive industry, early simulative prediction is desired for a short and cost-effective vehicle development. In terms of brake NVH, two basic computational methods can be distinguished, [17, p. 1206]:

- Time domain approaches
- (Linearized) stability analyses

Even if they feature promising capability for low-frequency brake phenomena such as creep groan, see e.g. [18], time domain approaches are typically limited to the application on strongly reduced systems for research due to the high computational effort. By contrast, linearized stability analyses in the form of the Complex Eigenvalue Analysis (CEA) are widely used for the prediction of higher-frequency squeal. Within this work, its ability to predict moan-related phenomena shall be investigated.

2. COMPLEX EIGENVALUE ANALYSIS

In this chapter, mathematical and theoretical essentials regarding the CEA in terms of its usage for brake NVH evaluation are explained, based on the more detailed contents of [19] and the authors' related publication, [13]. As large-scale simulations were carried out with the Finite Element solver PERMAS, some formulations relate to this software package, [20].

2.1. Theorem of Hartman and Grobman

Based on the theorem of Hartman and Grobman, the stability of a non-linear system near a fixed point can be determined by an evaluation of the linearized system: If the related eigenvalue has a non-zero real part, i.e. a so-called hyperbolic fixed point is existent, the stability behavior of linear and non-linear system are identical. This principle provides the theoretical basis for stability studies by CEA. [21]

2.2. Basic Equation and Procedure

Eventually, the dynamic system equation – typically given in modal coordinates – needs to be solved, see eq. 1.

$$\begin{aligned}\vec{0} = \widetilde{\boldsymbol{M}} \cdot \ddot{\vec{q}} + \\ \left[\widetilde{\boldsymbol{D}}_{\mathrm{V}} + \widetilde{\boldsymbol{D}}_{\mathrm{Ct}}(\Omega) + \widetilde{\boldsymbol{D}}_{\mathrm{G}}(\Omega)\right] \cdot \dot{\vec{q}} + \\ \left[\widetilde{\boldsymbol{K}}_{\mathrm{el}} + \widetilde{\boldsymbol{K}}_{\mathrm{Ct}} + \widetilde{\boldsymbol{K}}_{\mathrm{G}}(\Omega) + \widetilde{\boldsymbol{K}}_{\mathrm{C}}(\Omega) + \mathrm{i}\widetilde{\boldsymbol{H}}\right] \cdot \vec{q}\end{aligned} \quad (1)$$

In order to form this equation, an extensive model build-up consisting of several steps is necessary. This four-step process including its crucial simplifications is shown in fig. 3.

After finding the fixed point by application of a static, non-linear contact simulation in step 1, a (critical) linearization is performed. Here, the Coulomb sliding friction force within the disk/pad contact, relating to normal contact force, coefficient of friction and direction of the relative velocity according to eq. 2, is linearized by means of a Taylor series approximation.

$$\vec{f}_{\mathrm{R}} = -\mu \left\|\vec{f}_{\mathrm{N}}\right\| \frac{\vec{v}_{\mathrm{rel}}}{\left\|\vec{v}_{\mathrm{rel}}\right\|} \quad (2)$$

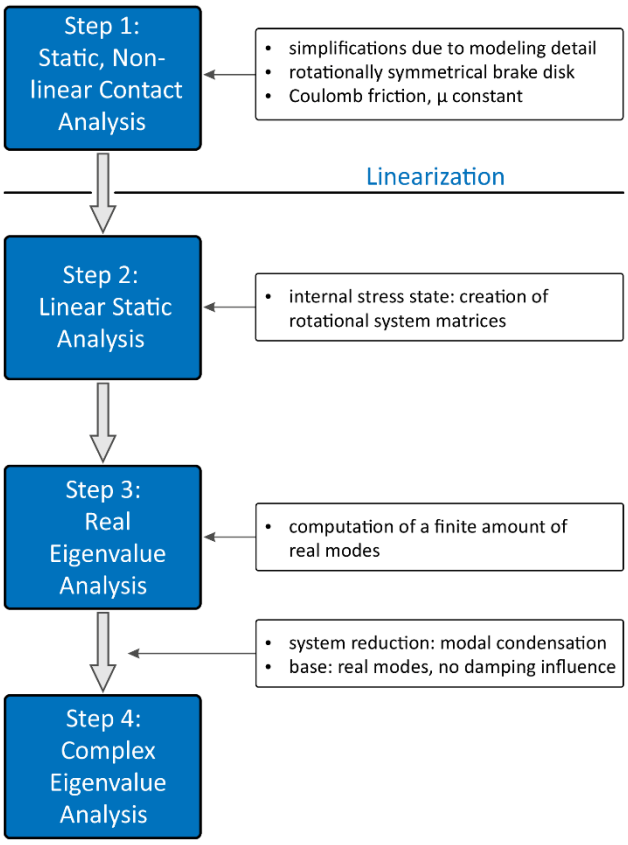

Fig. 3. Procedure for disk brake NVH Complex Eigenvalue Analysis, adapted from [13]

As presented within the related publication [13], the application of CEA is only meaningful for clearly non-zero relative speeds. Because of highly non-linear behavior near the state of sticking, predicted stability behaviors would be valid for exceptionally small intervals about the fixed point only. See fig. 4 for additional clarification.

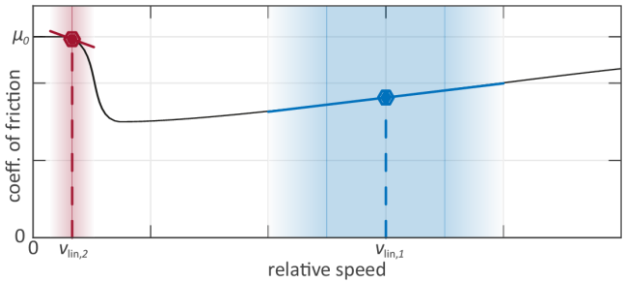

Fig. 4. Friction linearization at different fixed points, adapted from [13]

Especially for stick-slip-related creep groan phenomena, additional non-linearities such as e.g. elastomer bushing stiffnesses can be of influence, see [18]. Certainly, these effects are part of the linearization too.

Subsequently, supplemental rotational terms are created in a linear static analysis. On the one hand, geometric and convective stiffness contents relate to the square of the rotational speed. Especially for very low velocities, which are characteristic for creep groan and moan occurrence, these terms were found negligible according to [13]. On the other hand, linearly speed-dependent gyroscopic terms are known to alter the stability behavior even if the actual magnitude order is small, see e.g. [22, p. 143].

Due to a desired reduction of computational effort, the investigated vehicle corner Finite Element models are typically reduced based on a modal condensation. Therefore, real modes – without the influence of damping – are computed to assemble a new, smaller set of basis (eigen)vectors $\boldsymbol{\Phi}$. See eq. 3 and eq. 4.

$$[\boldsymbol{K}_{\mathrm{el}} - \omega^2 \boldsymbol{M}] \cdot \vec{\phi} = \vec{0} \tag{3}$$

$$\boldsymbol{\Phi} = \left[\vec{\phi}_1, \vec{\phi}_2, \ldots, \vec{\phi}_{\mathrm{n}}\right] \tag{4}$$

Eventually, the coordinate transformation and a left multiplication by the transposed modal matrix $\boldsymbol{\Phi}^{\mathrm{T}}$ according to eq. 5 leads to the equation to solve, eq. 1.

$$\underbrace{[\boldsymbol{\Phi}^{\mathrm{T}} \boldsymbol{M}\, \boldsymbol{\Phi}]}_{\hat{\boldsymbol{M}}} \cdot \ddot{\vec{q}} + \underbrace{[\boldsymbol{\Phi}^{\mathrm{T}} \Sigma \boldsymbol{D}_i\, \boldsymbol{\Phi}]}_{\hat{\boldsymbol{D}}} \cdot \dot{\vec{q}} + \underbrace{[\boldsymbol{\Phi}^{\mathrm{T}} \Sigma \boldsymbol{K}_i\, \boldsymbol{\Phi}]}_{\hat{\boldsymbol{K}}} \cdot \vec{q} = \vec{0} \tag{5}$$

By usage of a complex approach consisting of complex eigenvector and complex eigenvalue as in eq. (6), the equation then is solved.

$$\vec{q} = \vec{\phi}_{\mathrm{c}} \cdot \mathrm{e}^{(\delta + \mathrm{i}\omega_{\mathrm{c}})t} \tag{6}$$

In terms of stability, the equivalent viscous damping ratio is typically evaluated. This characteristic number, given in eq. (7), indicates unfavorable, unstable behavior by a negative sign related to the eigenvalue's real part.

$$\xi_i = \frac{-\delta_i}{\delta_i^2 + \omega_{\mathrm{c},i}^2} \tag{7}$$

It has to be noted that this value only relates to the stability about the fixed point computed in step 1, no conclusion about resulting oscillation amplitudes can be drawn by the CEA. One big drawback of this method is the fact that stability is regularly over- or underestimated in industrial applications. Nevertheless, CEA is capable to efficiently handle large parameter variations, which is an important reason for its wide usage.

2.3. Application for Brake Moan

As stated above, the application of CEA for predictive brake NVH evaluation is only meaningful for clearly non-zero relative speeds. In terms of brake moan, this corresponds to phenomena which occur in the relevant

frequency range and are rather excited by modal coupling than by global stick-slip transitions in the disk/pads contact zones. If this is the case, moan can be assumed as a dynamic instability or a kind of "low-frequency brake squeal": Based on [2] and the related work [13], CEA stability analysis should be applicable.

3. SIMULATIVE INVESTIGATIONS

3.1. Model Description

Starting from a Finite Element model provided by an industrial project partner, a full corner model appropriate for moan evaluation was built up. In this case, two different rim designs were compared. Within [13], this model's predecessor is explained.

As one can see in fig. 5 and fig. 6, the corner model features all main components between wheel contact point and chassis of the car. This includes the fixed caliper brake system with brake disk, caliper and pads as well as the double wishbone suspension with wheel carrier and steering link. Anti-roll bar and drive shaft were removed due to the corresponding experimental setup.

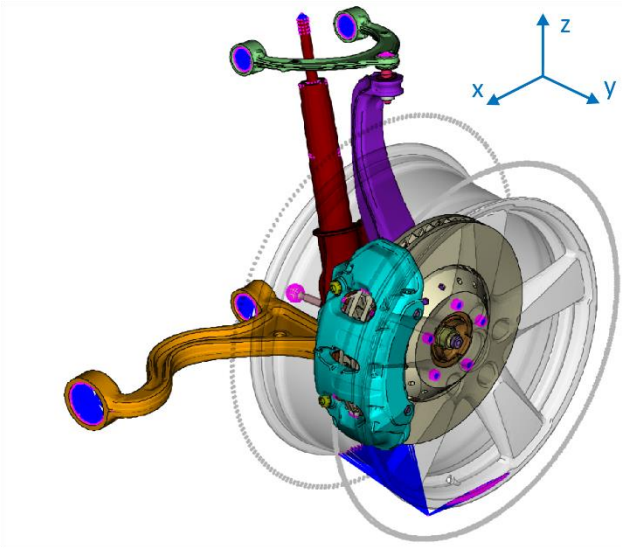

Fig. 5. Investigated Finite Element model with rim A, [16]

Furthermore, a rim model consisting of 2nd order tetrahedron elements in combination with mass points representing the tire inertia and a three-dimensional stiffness/damping element in the wheel contact point introduce wheel influences. Two different rim designs were compared: Rim A with 5 separate, broader spokes and rim B with 20 slim spokes – see fig. 5 and fig. 6 for a depiction. Regarding the mass moment of inertia about the wheel axis, a swing experiment delivered rather accurate values of rim A. For rim B, identical rotational inertia was assumed and introduced by arranging the tire mass points' radial center distance accordingly.

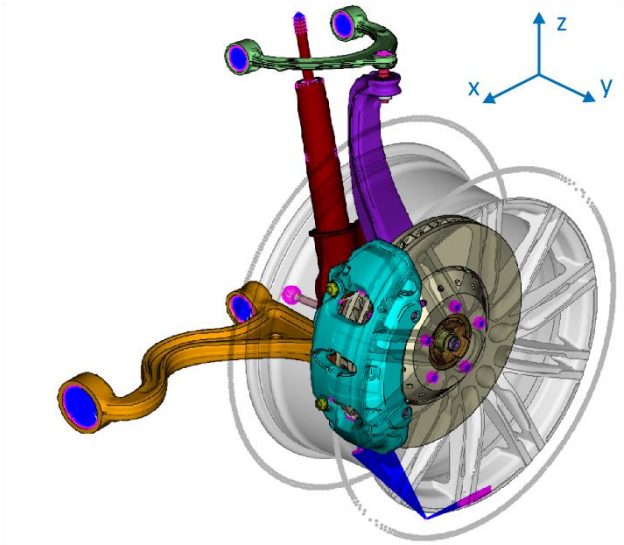

Fig. 6. Investigated Finite Element model with rim B, [16]

Depending on rim design, the overall number of nodes was 690 000 (rim A) and 1 000 000 (rim B) respectively. Boundary conditions were applied at the interfaces to the chassis in Degrees of Freedom (DOFs) 123456 and at the wheel contact point with the road surface (DOFs 123). Moreover, the steering link was supported translational and in one torsional rotation direction (local DOFs 1235).

Compared to the model presented in [13], measures were taken to improve its ability for predicting moan phenomena: Firstly, less damping was introduced at the wheel contact point. Secondly, rim nodes of the Multi-Point Constraint connecting the rim to the ground were reduced. Thirdly, real modes were computed up to a higher frequency of 2.5 kHz.

Operational parameters can be found in table 1. Even though moan can occur also at slightly higher speeds and even lower brake pressures, it basically emerges in operating ranges similar to creep groan, [1, p. 630, 23]. Hence, parameters were chosen in the low brake pressure / low vehicle speed range identical to [13], which also corresponds to experimental test results.

Brake pressure p_B	4 - 16 bar	Δ 2 bar
Vehicle speed v_{veh}	0.04 - 0.4 km/h	Δ 0.004 km/h
Coeff. of friction μ	0.25 - 0.55	Δ 0.05

Table 1. Simulative parameter variation ranges

Within [13] and [18], influences of non-linear elastomer bushing stiffness and damping behavior were proven to be highly relevant for low-frequency creep groan. As the study presented here builds up on a corresponding model, these parameters were modeled with special care: E.g.,

bushing stiffnesses were implemented in a non-linear parameter-dependent manner. However, the results reveal less relevance for moan, hence, a detailed explanation regarding these aspects is not featured here.

3.2. Simulative Results

In the following, CEA was performed for both rim designs using a vehicle reference speed of 0.2 km/h – rotational terms vary for deviations. Modal displacements as well as eigenfrequency and stability behavior were evaluated. Therefore, depictions of modal displacements and multi-dimensional stability diagrams are shown.

For rim A, only one moan-relevant mode was found unstable. Within fig. 7, its displacements are shown: Torsion between wheel hub and the rim's outer part dominates the oscillation. Furthermore, higher order bending modes of the control arms and the spring with damper assembly can be detected.

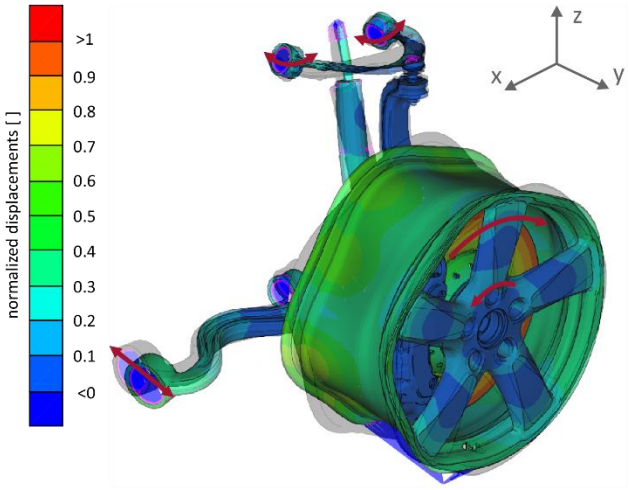

Fig. 7. Normalized displacements of the (partly unstable) moan-relevant mode with rim A for μ=0.55 and p_B=10 bar, adapted from [16]

Fig. 8 shows the corresponding eigenfrequency and stability behavior. This diagram contains 7 surfaces, drawn over the whole parameter range of brake pressures and vehicle speeds as x- and y-axis. Each of these surfaces is related to a coefficient of friction. Moreover, the vertical coordinate of each surface point corresponds to the resulting eigenfrequency. In addition, another dimension is introduced by color: unstable parameter combinations are marked blue, depending on the equivalent viscous damping ratio. Stable zones remain white.

In fig. 8, only one parameter combination was computed unstable, recognizable by the slightly blue color zone at the operating point μ=0.55, p_B=10 bar and v_{veh}=0.04 km/h. Generally, eigenfrequency was in the range of 562.5 – 563.4 Hz, changing only little for different parameters. Nonetheless, two combinations of brake pressure and coefficient of friction, including the unstable spot, feature slightly lower frequencies.

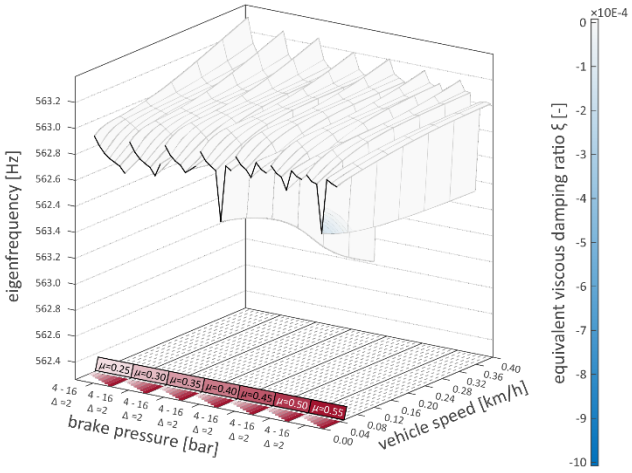

Fig. 8. Multi-dimensional stability diagram for the torsional rim mode with rim A, adapted from [16]

For rim B, no unstable mode was found within the moan-relevant frequency range at all. However, due to the resulting mode with rim A and experimental/literature results according to chapter 4, a torsional rim mode was evaluated. Fig. 9 shows the mode's displacements: By contrast to the mode with rim A, bending of suspension components such as control arms or spring with damper assembly cannot be found here.

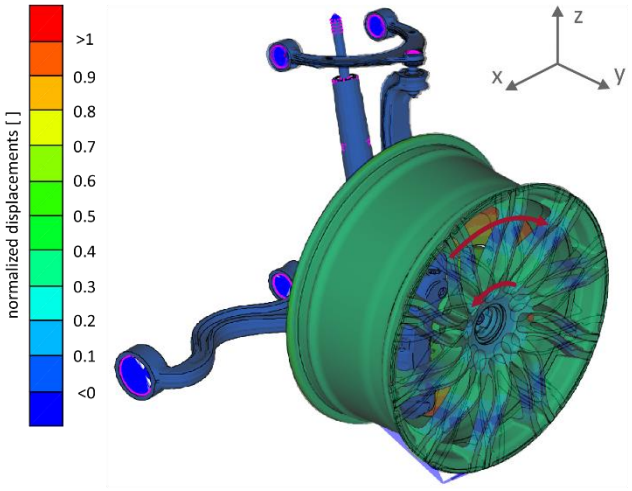

Fig. 9. Normalized displacements of the (stable) moan-relevant mode with rim B for μ=0.4 and p_B=16 bar, adapted from [16]

Fig. 10 shows no unstable parameter points for rim B. Furthermore, frequency changed only in its third decimal place in the whole parameter range at approx. 358.7 Hz.

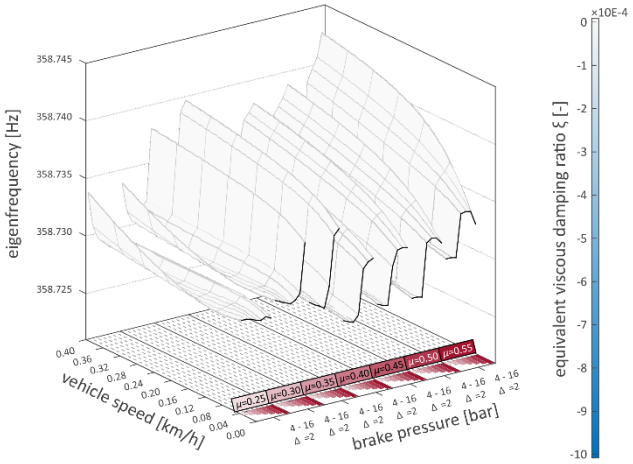

Fig. 10. Multi-dimensional stability diagram for the torsional rim mode with rim B, adapted from [16]

4. EXPERIMENTAL VALIDATION

For validation, experimental tests were performed on a drum-driven suspension and brake test rig. An example setup can be seen in fig. 11. By use of special adapters, the components of the vehicle's front left corner were mounted to the test bench plate according to the real vehicle. Analogously to the simulative investigations, anti-roll bar and drive shaft were omitted.

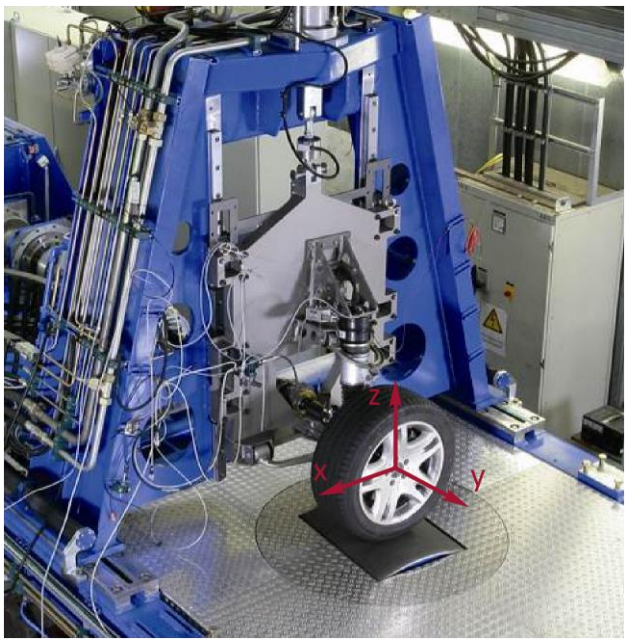

Fig. 11. Exemplary setup on the combined suspension and brake test rig at FTG / Graz University of Technology, adapted from [13]

During the tests, certain brake pressure and speed profiles according to [24] were retraced by the hydraulic unit and the speed-controlled drum. The coefficient of friction between disk and pads was estimated at approx. 0.35 by a method described within [25]. Furthermore, effects resulting from the vehicle's unladen weight were considered via a vertical pre-tension by a hydraulic cylinder.

In the following, data from several pad acceleration sensors and an incremental rotary encoder sampled with 10 kHz was used for the evaluation of dominant frequencies as well as relative speeds at the theoretic friction radius. The sensor positions can be found in fig. 12, details about measurement and procedure are given within [26].

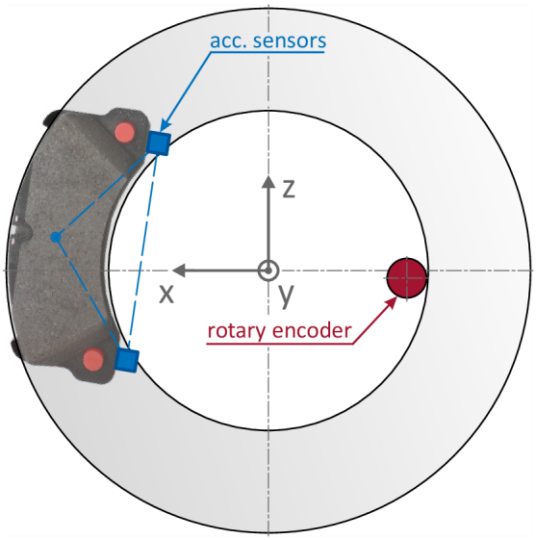

Fig. 12. Approximated sensor positions for acceleration measurement and evaluation of relative speed, adapted from [16]

In addition to the in-house experiments, literature results of similar or even nearly identical setups were consulted for validation purposes. Within [14], a project partner's work on an almost identical system is described.

4.1. Moan-Relevant Mode for Rim A

According to the simulative investigations, unstable behavior could probably occur in case of high coefficients of friction, moderate brake pressures and very slow speeds. However, as already mentioned in [13], moan was not found on the test bench for this rim.

What is more, personal correspondence with the main author of [14] further emphasized this setup's moan stability. Nonetheless, a noise phenomenon of almost identical frequency was said to be 'enforced' on test bench by this project partner. In addition, the torsional rim mode was verbally confirmed.

Interestingly, simulations have predicted a strongly parameter-dependent moan occurrence. However, this contradicts the theory of a dynamic instability, see [2].

4.2. Moan-Relevant Mode for Rim B

The torsional rim mode at approx. 358.7 Hz was computed stable for all parameter combinations. Even in an increased parameter range with coefficients of friction from 0.25 – 0.8, no unstable operating points were found. By contrast, experiments with this setup revealed moan oscillations at an approximately similar frequency of 386 Hz, see already published results within [13] and [26].

Meaningful averaging, filtering and integration of the signals from rotary encoder and acceleration sensors led to an evaluation of tangential velocities at the theoretic friction radius, [13]. The lower subfigure in fig. 13 displays constantly positive relative speed between brake disk and pads during moan operation. This relates to a dynamic instability and points out the principal capability of CEA prediction for this moan phenomenon.

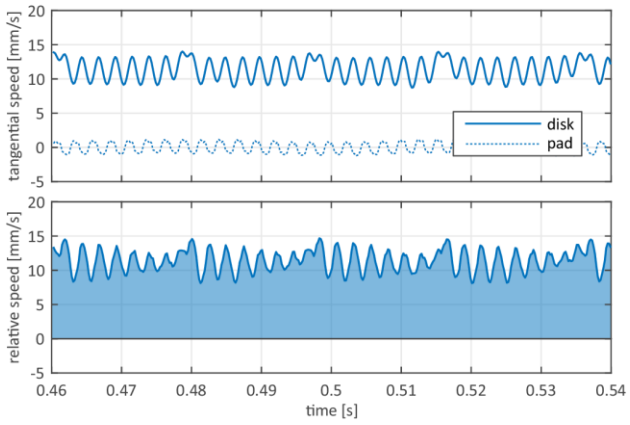

Fig. 13. Tangential disk/pad speeds and resulting relative speed during 386 Hz moan action, adapted from [13]

Furthermore, fig. 2 displays a time and a frequency plot of the longitudinal pad acceleration for this moan effect.

Within [14], a moan mode consisting mainly of torsional rim displacement was measured via laser vibrometry for an almost identical system. Here, the frequency found at 512 Hz was essentially higher, probably due to a different slim-spoke rim design.

5. CONCLUSION

Test bench experiments have shown, that brake NVH phenomena within a frequency range related to the so-called moan can (in the present case) be described by a dynamic instability. Hence, the linearizing CEA should be able to predict possibly critical eigenmodes.

However, simulative investigations of two different rim designs within a chosen parameter range of low brake pressures and vehicle speeds have delivered a stability behavior exactly opposite to the real-world behavior: Whereas rim A was computed unstable at least for one parameter set, rim B was predicted stable.

Most probably, this discrepancy results from an insufficient Finite Element model: Due to modal deflections, it can be assumed that a more sophisticated tire model paired with the implementation of more accurate parameters is necessary. Because of their high influence on stability behavior, damping influences resulting from elastomer bushings could also be a starting point, see [27, pp. 524-525]. In addition, more detailed treatment of the tribological contact, e.g. by augmented state vectors as explained in [17] or an improved condensation method according to [28], could alter the simulative output in a positive manner.

Nonetheless, the computed torsional rim modes and their influence on the dominant moan frequency were in good correspondence with tests performed on similar or even almost identical systems.

6. REFERENCES

[1] B. Breuer and K. H. Bill, Eds.: ***Bremsenhandbuch: Grundlagen, Komponenten, Systeme, Fahrdynamik,*** 5th ed., Wiesbaden, Springer Fachmedien, 2017.

[2] J. Bauer, M. Körner, and A. Pfaff: **Moan Noise - The Phenomenon and Solution Approaches,** *EuroBrake 2017: Conference Proceedings*, Dresden, 2017.

[3] Y. Dai, T. C. Lim: **Suppression of brake squeal noise applying finite element brake and pad model enhanced by spectral-based assurance criteria,** *Applied Acoustics*, vol. 69, no. 3, pp. 196–214, 2008, DOI: 10.1016/j.apacoust.2006.09.010.

[4] D. Wallner: ***Experimental and numerical investigations on brake squeal: Development of a smart friction force measuring sensor,*** Dissertation, Graz, Verl. der Techn. Univ. Graz, 2013.

[5] R. Allgaier: ***Experimentelle und numerische Untersuchungen zum Bremsenquietschen,*** Dissertation, Düsseldorf, VDI-Verlag, 2002.

[6] R. Nunes, A. Shivaswamy, and M. Könning: **A Time Domain Approach Towards Analysing Creep Groan Noise in Automobile Brakes,** *EuroBrake 2016: Conference Proceedings*, Milan, Italy, 2016.

[7] C. Bittner: ***Reduzierung des Bremsrubbelns bei Kraftfahrzeugen durch Optimierung der Fahrwerkslagerung,*** Dissertation, Technical University of Munich, Munich, Germany, 2006.

[8] J. Wallaschek, K.-H. Hach, U. Stolz, and P. Mody: **A Survey of the Present State of Friction Modelling in the Analytical and Numerical Investigation of Brake Noise Generation,** *Proceedings of the ASME Design Engineering Technical Conferences:* Las Vegas, NV, USA, 1999, pp. 2299–2310.

[9] Y. D. Kim et al.: **Identification of moan-noise generation mechanisms by an experimental method and verification of the mechanism by finite element analysis,** *Proceedings of the Institution of Mechanical Engineers, Part D: Journal of Automobile Engineering*, vol. 229, no. 10, pp. 1392–1405, 2015, DOI: 10.1177/0954407014562618.

[10] A. Wang, L. Zhang, N. Jaber, and J. Rieker: **On Brake Moan Mechanism from the Modeling Perspective,** *SAE Technical Papers*, 2003, DOI: 10.4271/2003-01-0681.

[11] M. Donley, D. Riesland: **Brake groan simulation for a McPherson strut type suspension,** *SAE Technical Papers*, 2003, DOI: 10.4271/2003-01-1627.

[12] H. Marschner, P. Leibolt, A. Pfaff, and C. Morschel: **Untersuchung der Wirkmechanismen reiberregter Haft-Gleit-Schwingungen am Beispiel des Bremsenknarzens und analoger Schwingungsphänomene,** *XXXV. Internationales µ-Symposium - Bremsen-Fachtagung:* Bad Neuenahr, pp. 84–104, 2016.

[13] S. Huemer-Kals, M. Pürscher, and P. Fischer: **Application Limits of the Complex Eigenvalue Analysis for Low-Frequency Vibrations of Disk Brake Systems,** *SAE Technical Papers*, 2017, DOI: 10.4271/2017-01-2494.

[14] D. Müller, D. Wallner, S. Carvajal, and F. Gauterin: **Simulation der Frequenzantwort des Rad-Bremse Verbundes auf gemessene Anregungssignale,** *18. Kongress SIMVEC - Simulation und Erprobung in der Fahrzeugentwicklung: Berechnung, Prüfstands- und Straßenversuch*, Baden-Baden, pp. 491–508, 2016.

[15] A. K. Kléperon, R. D. Abreu, R. M. Bitencourt, and F. J. Almeida: **Brake Moan Noise Study through Experimental and Operational Modal Analysis Techniques in a Passenger Car,** *SAE Technical Papers*, 2014, DOI: 10.4271/2014-36-0768.

[16] S. Huemer-Kals: ***Complex Eigenvalue Analysis of Friction Induced Low-Frequency Vibrations in Vehicle Disc Brake Systems,*** Master Thesis, Institute of Automotive Engineering, Graz University of Technology, 2018.

[17] A. Völpel, G. P. Ostermeyer: **Investigation of the Influence of ODE Based Friction Models on Complex FEM Brake Models in the Frequency Domain,** *SAE International Journal of Passenger Cars - Mechanical Systems*, vol. 9, no. 3, pp. 1206–1213, 2016, DOI: 10.4271/2016-01-1931.

[18] M. Pürscher, S. Huemer-Kals, and P. Fischer: **Experimental and Simulative Study of Creep Groan in Terms of MacPherson Axle Bushing Elasticities,** *EuroBrake 2018: Conference Proceedings*, The Hague, 2018.

[19] N. Gräbner: ***Analyse und Verbesserung der Simulationsmethode des Bremsenquietschens,*** Dissertation, Technische Universität Berlin, Berlin, 2016.

[20] INTES GmbH: ***PERMAS-Workshop - Dynamik II: Erweiterungen und spezielle Anwendungen,*** Stuttgart, Germany, Oct. 2015.

[21] J. Guckenheimer, P. Holmes: ***Nonlinear oscillations, dynamical systems, and bifurcations of vector fields,*** 7th ed., New York, NY, USA, Springer, 2002.

[22] Hartmut Hetzler: ***Zur Stabilität von Systemen bewegter Kontinua mit Reibkontakten am Beispiel des Bremsenquietschens,*** Dissertation, Karlsruhe, Universitätsverlag Karlsruhe, 2008.

[23] B. Siegl: **Output-only Modal Analysis for System Identification Before Brake Squeal,** *presented at ISNVH 2018*, Graz, Austria, Jun. 22, 2018.

[24] M. Pürscher, P. Fischer: **Systematic Experimental Creep Groan Characterization Using a Suspension and Brake Test Rig,** *SAE Technical Papers*, 2017, DOI: 10.4271/2017-01-2488.

[25] M. Pürscher, P. Fischer: **Strain Gauge Application at Pad Backing Plates to Investigate Friction Force and NVH Issues,** *EuroBrake 2017: Conference Proceedings*, Dresden, 2017.

[26] M. Pürscher, S. Huemer-Kals, and P. Fischer: **Experimental Investigation of Low-Frequency Vibration Patterns in Automotive Disk Brake Systems: Utilization Study for Modal Simulation Methods,** *SAE Technical Papers*, 2018, DOI: 10.4271/2018-01-1513.

[27] N. Hoffmann, L. Gaul: **Effects of damping on mode-coupling instability in friction induced oscillations,** *ZAMM - Zeitschrift für Angewandte Mathematik und Mechanik*, vol. 83, no. 8, pp. 524–534, 2003, DOI: 10.1002/zamm.200310022.

[28] N. Gräbner, S. M. Quraishi, C. Schröder, V. Mehrmann, and U. von Wagner: **New numerical methods for the complex eigenvalue analysis of disk brake squeal,** *EuroBrake 2014: Conference Proceedings*, Lille, France, 2014.